HEFAT2007
5th International Conference on Heat Transfer, Fluid Mechanics, and Thermodynamics
1-4 July 2007, Sun City, South Africa
Paper Number: PD1

AN IMMERSED BOUNDARY METHOD ON CARTESIAN MESH WITH LOCAL REFINEMENT APPLICED TO HEAT CONVECTIONN PROBLEMS

Dartzi Pan and Tzung-Tza Shen
Department of Aeronautics and Astronautics
National Cheng Kung University
Tainan, Taiwan, ROC
e-mail: dpan@mail.ncku.edu.tw

ABSTRACT

The incompressible Navier-Stokes equations with heat transfer are solved by an implicit pressure correction method on Cartesian mesh with local refinement. A simple immersed boundary method is developed to treat arbitrary solid bodies in the flow field. A direct forcing term was added to cells inside the immersed body to enforce the Dirichlet boundary condition for velocity and temperature. This forcing is also assumed to have an active range of one cell size normal to the immersed boundary, acting on fluid cells external to the immersed body. For those cells within the active range, the forcing term is scaled by the normal distance from the cell center to the body surface. The same pressure Poisson equation is applied to the entire flow field without distinguishing whether it is inside or outside the immersed body. Various tests are computed to verify this simple immersed boundary method, including the steady and unsteady forced convection over a circular cylinder and the natural convection over a heated circular cylinder inside a square cavity.

INTRODUCTION

Recently numerical methods for solving incompressible flows on fixed Cartesian grids are gaining popularity for their relative ease in treating complex immersed bodies [1-10]. The differences among these methods lie on the different ways the boundary conditions for the immersed bodied are enforced. For example, the immersed boundary method [1] and the virtual boundary method [2] simulate the no-slip boundary condition on the body surfaces by adding appropriate forcing terms to the appropriate cells. The force added to the flow field is spread over several grid cells using a delta function-like distribution normal to the fluid-solid interface. In the direct-forcing method [4, 5] the no-slip condition at the fluid-solid interface is used to interpolate the velocity distribution for cells around the solid body without actually solving the fluid equations. The fictitious domain method [6] is a finite-element method that enforces the no-slip boundary condition using Lagrange multiplier.

Very recently, Pan [7,8] viewed the domain inside the solid body as being occupied by the same fluid as outside with a prescribed divergence-free velocity field. In this view a fluid-body interface is similar to a fluid-fluid interface commonly encountered in the Volume of Fluid (VOF) method for the two-fluid flow problems. Thus a Volume of Body (VOB) function analogous to the VOF function can be used to identify and track the presence of the immersed body. For the grid cells containing the fluid-body interface, a mixture of the "two fluids" based on the fluid volume is assumed. This volume averaging of the velocity automatically enforces the no-slip boundary condition inside the interface cell, but it also smears the fluid-body interface to the size of one cell width. In this work, we tried to improve the representation of the fluid-body interface by using a scaled forcing term. A direct forcing is added to cells inside the body to enforce the Dirichlet boundary condition for the velocity and temperature. This forcing is further assumed to have an effective range of one cell size normal to the body surface, acting on cells external to the immersed body. For those cells within the active range, the amount of added forcing is scaled by a Delta function based on the normal distance from the cell center to the body surface. Test results of this simple scaled direct forcing method are reported in this paper**,** including the steady and unsteady forced convection over a circular cylinder and the natural convection over a heated circular cylinder inside a square cavity**.**

IMPLICIT PRESSURE CORRECTION METHOD

The incompressible Navier-Stoked equations with heat transfer can be written as

$$\begin{aligned}
&\oint_{CS}\vec{v}\cdot d\vec{S}=0\\
&\frac{\partial}{\partial t}\int_{CV}\vec{v}dV+\oint_{CS}\vec{v}\vec{v}\cdot d\vec{S}-\oint_{CS}\frac{1}{Re}\vec{\nabla}\vec{v}\cdot d\vec{S}+\int_{CV}\frac{\vec{Gr}}{\mathrm{Re}^2}\theta dV\\
&\qquad\qquad+\oint_{CS}Pd\vec{S}=0\\
&\frac{\partial}{\partial t}\int_{CV}\theta dV+\oint_{CS}\theta\vec{v}\cdot d\vec{S}-\oint_{CS}\frac{1}{PrRe}\vec{\nabla}\theta\cdot d\vec{S}=0
\end{aligned}\qquad(1)$$

where $\vec{v}$, P and θ are Cartesian velocity vector, pressure and temperature, respectively; *Re* is the Reynolds number; *Pr* is the Prandtl number; $\vec{Gr}$ is the vector of Grashof number representing the thermal buoyancy; *CV* is the control volume considered and *CS* is the boundary surface of *CV*. Applying the Divergence theorem, adapting the backward time differencing

scheme and keeping the pressure fixed at the current time level *n*, the momentum and temperature equations can be discretized as:

$$(\frac{c_1Q^* - c_2Q^n + c_3Q^{n-1}}{\Delta t} + R^*_{inv} - R^*_{vis} + H^* + R^n_P)\Delta V = 0 \quad (2)$$

where the superscript "*" represents the intermediate state, "*n*" the current time level; ΔV is the volume of the considered cell; Δt is the time increment. The vector of conserved variables is defined as $Q = [u \quad v \quad \theta]^T$. R_{inv}, R_P and R_{vis} are the surface integral of inviscid flux, the pressure flux, the viscous flux divided by the cell volume, respectively, *H* is the source term. The constants are c_1*=1.5,* c_2*=2* and c_3*=0.5* for the second-order backward differencing scheme, and c_1*=1,* c_2*=1* and c_3*=0* for the first order Euler implicit scheme. The velocity $\vec{v}^*$ generally does not satisfy the divergence-free condition. The velocity and the pressure are corrected as

$$\vec{v}^{n+1} = \vec{v}^* - \Delta t\vec{\nabla}\phi^n \qquad P^{n+1} = P^n + \phi^n \quad (3)$$

where ϕ is the pressure correction. By requiring $\vec{v}^{n+1}$ be divergence-free, we obtain the Poisson equation [7-9]:

$$\nabla^2\phi^n - \frac{\vec{\nabla}\cdot\vec{v}^*}{\Delta t} = 0 \quad (4)$$

After obtaining $\vec{v}^{n+1}$ and p^{n+1}, the temperature equation alone in Eq. (2) is then solved to update the temperature, with θ^* in the equation being replaced by θ^{n+1} and $\vec{v}^*$ and p^n being replaced by the latest $\vec{v}^{n+1}$ and p^{n+1}. Equations (2), (3) and (4) and the final temperature update constitute the implicit fractional step pressure-correction method used in this work**.**

FINITE VOLUME DISCRETIZATION

A finite volume method [7,8] based on the integral form of Eq. (1) is used to discretize the momentum equation on a cell-centered unstructured Cartesian grid system. The variable states at the cell faces are linearly reconstructed from the center values. The convective fluxes are upwind oriented based on the velocity at the cell face. The pressure force is computed using the reconstructed pressure state at the cell face, while the viscous fluxes are computed using the velocity gradients at the cell face. Overall, a second order accurate upwind difference scheme is used for the convective fluxes and central difference schemes are used for the pressure and viscous fluxes. To compute the divergence of velocity, a normal face velocity is defined separately from the cell center velocity. A fourth derivative of pressure is added in the divergence field through the normal face velocity. This face velocity is corrected in a similar fashion as Eq. (3), and thus constructing the discretized Poisson equation for the pressure correction. The technique of sub-iteration is employed for time accuracy, and an implicit multi-grid method is developed to accelerate the convergence of the inversion process. Also, a similar implicit multi-grid method is developed to solve Eq. (4), or the pressure Poisson equation.

SCALED DIRECT FORCING

The position, the velocity $\vec{v}_B$ and the temperature θ_B of the immersed bodies are assumed known from some appropriate governing equations. The body velocity $\vec{v}_B$ is assumed to be divergence-free, such that the pressure field inside the body surface obeys the same governing equation as the pressure field outside. Under this assumption, Eq. (4) can be applied to the entire computational domain including the body interior.

The current immersed boundary method simulates the existence of solid body by adding a direct forcing term to the governing equations:

$$\frac{c_1Q^* - c_2Q^n + c_3Q^{n-1}}{\Delta t} + R^*_{inv} - R^*_{vis} + H^* + R^n_P + f_{IBM} = 0 \quad (5)$$

The modeling of f_{IBM} constitutes the major difference among various immersed boundary methods. In this work, it is assumed that f_{IBM} depends on the normal distance r_n of a cell center to the body surface, where $r_n > 0$ indicates the body exterior, $r_n < 0$ indicates the body interior and $r_n = 0$ indicates the body surface.

For cell centers inside the body surface with $r_n < 0$, the working of f_{IBM} should enforce the known boundary conditions, resulting the following forcing term for each body cell

$$f_{IBM} = -(\frac{c_1Q^{n+1}_B - c_2Q^n + c_3Q^{n-1}}{\Delta t} + R^*_{inv} - R^*_{vis} + H^* + R^n_P) \quad (6)$$

where $Q_B = [u_B \quad v_B \quad \theta_B]^T$ represents the component of body velocity and the body temperature at the new time level *n+1*. Note that if Neumann boundary condition is set for temperature, then θ_B should be interpoated from the surrounding fluid temperature using given temperature gradient. For a cell center on or external to the body surface with $r_n \geq 0$, it is assumed that the forcing added to the cell center depends on its project point on the body surface and can be represented by

$$f_{IBM,Pj} = -\phi_{SDF}(\frac{c_1Q^{n+1}_B - c_2Q^n + c_3Q^{n-1}}{\Delta t} + R^*_{inv} - R^*_{vis} + H^* + R^n_P)_{Pj} \quad (7)$$

where the subscript "*Pj*" indicates the projection point on the surface for the cell center under consideration. The coefficient ϕ_{SDF} is a numerical Delta function given by

$$\phi_{SDF} = \begin{cases} \frac{1}{2}\left(1+\cos(\pi\frac{r_n}{\eta})\right), & 0 \le r_n/\eta \le 1 \\ 0, & r_n/\eta > 1 \end{cases} \quad (8)$$

where η is a preset effective length of $f_{IBM,pj}$, whicht is chosen to be the minimum cell size $\ell_{\min}$ of the mesh. Not that the condition of $\phi_{SDF}=1$ when $r_n=0$ will enforce the Dirichlet boundary condition on the body surface, and the condition of $\phi_{SDF}=0$ when $r_n \ge \eta$ indicates that no forcing is added when the cell is one cell size away from the body surface. Generally, the projection point does not coincide with the cell center and the terms inside the brackets of Eq. (7) need to be estimated using nearby cell center values. In this work, we choose a bilinear interpolation based on the cell center values surrounding the projection point. Note that here $\vec{f}_{IBM,p}$ is similar to the Lagrangian force developed in the Physical Virtual Model (PVM) of Silva et al. [12].

FORCE CALCULATION

To compute the aerodynamic forces acting on the immersed body and the total heat transfer over the body surface, the surface integral of pressure and viscous stress is needed:

$$\vec{f}_{Body} = \sum_{surface}(-P\Delta\vec{S} + \frac{1}{Re}\vec{\nabla}\vec{v}\cdot\Delta\vec{S})$$

$$H_{Body} = \sum_{surface}\frac{1}{PrRe}\vec{\nabla}\theta\cdot\Delta\vec{S} \quad (9)$$

where the summation is performed on all surface elements of the body surface. The pressure at each surface element center is obtained by a bilinear interpolation based on the vertex values of the cell containing the surface element center. The variable gradient for a surface element, however, is not estimated at the element center in this work, but at a point having a normal distance $0.5\,\ell_{\min}$ away from the surface element. In other words, the variable gradient is estimated at a point on the $\phi_{SDF}=0.5$ contour closest to the element center under consideration. This choice is based on the assumption that the variable gradient can be accurately estimaed at the middle of the transition zone between body surface and the outside flow field.

FORCED CONVECTION OVER A CYLINDER

The steady and unsteady flows over a circular cylinder of unit diameter at *Re*=40 and 100 are computed on an unstructured Cartesian grid. The grid shown in Fig. 1(a) is refined around the cylinder to have about 384 cells containing the cylinder surface. The downstream boundary follows the upwind differenced equation of $(\partial\vec{v}/\partial t)+U_n(\partial\vec{v}/\partial x)=0$, where U_n is the normal outflow velocity at the boundary.

For the steady case of *Re*=40, the Euler implicit method is used with the maximum CFL number around 20. The infinity norm of the steady state residual for $\phi_{SDF}=0$ cells, or the terms in Eq. (2) without involving Δt, dropped 4 orders of magnitude in 500 steps. The computed streamlines are plotted in Fig. 1(b). For convenience, the contour of $r_n=0$ is displayed as the cylinder wall. The streamlines around the cylinder are smooth, indicating the effects of the interface cells in smoothening the zigzag representation of the cylinder surface. Figure 2(a) shows the computed pressure contours. Note that the pressure inside the cylinder adjusts itself automatically to the pressure field outside. The pressure contours intersect the cylinder wall in a nearly orthogonal manner. The pressure coefficient at the intersection of the cylinder surface and the grid lines is interpolated using the surrounding center values and plotted in Fig. 2(b). The data from Fornberg [11] are also included for comparison. The two results generally agree with each other very well. For the unsteady case of *Re*=100, the second order backward difference scheme is used for time integration. The time increment is chosen such that the expected vortex shedding cycle takes about 50 time steps to complete. The instantaneous streamlines at certain instant in the periodic vortex shedding process are plotted in Fig. 3(a). The vorticity contours are shown in Fig. 3(b). The unsteady vortex shedding behind the cylinder is clearly seen. Table I lists the computed lift coefficient *(Cl)*, drag coefficient *(Cd)*, the wake length (*Lw*) normalized by the diameter *(d)*, the Strauhal number *(St)* of unsteady vortex shedding and the averaged Nusselt number *Nu* over cylinder surface. The comparisons between the present work and the work of others are generally satisfactory. The curve fit of experimental data for average Nusselt number in Holman [12] is used as reference data. The difference between the computed *Nu* and the experimental curve fit is less than *5%*.

NATURAL CONVECTION OVER A HEATED CYLINDER IN CAVITY

The next validation examines the natural convection heat transfer from a heated cylinder placed in a square cavity of unit length. This problem has been studied by Moukalled and Darwish [13] and Sadat and Couturier [14]. The radius of the cylinder is *0.1*. The temperature of the cylinder is one and the wall temperature is zero. The center of the cylinder is at *(0.35, 0.35)* from the left lower corner of the cavity. The natural convection with Rayleigh number $Ra=10^4$, 10^5 and 10^6 are computed. Four levels of refinement on a 64×64 grid are employed, resulting the finest cell length of *1/1024*. The total number of cells for the fine mesh is *13036*, which is about *3.2* times of that of the base mesh. The number of interface cells is about *577*, which is about *17.5* times of that of the base mesh. This indicates the advantage of local refinement on the unstructured Cartesian mesh.

Table 2 lists the computed average Nusselt number over the hot cylinder and the published data in Ref. [13] and [14]. The agreement with the publish data is generally very good. Figure 4 shows the computed streamlines and isotherms. The streamlines and isotherms are similar to those presented in Ref. [13, 14]. The formation of a thermal plume at $Ra=10^6$ is clearly observed.

CONCLUSIONS

A simple immersed boundary method on unstructured Cartesian meshes is developed and tested for incompressible flows with immersed bodies. The solid body is modeled by a direct forcing term added to the governing equations. For cell centers inside the solid body, this forcing term enforces the Dirichlet boundary condition directly. For cells external to the body within an effective range, this forcing term is scaled by the normal distance from the cell center to the body surface. The same pressure Poisson equation applies to the entire computational domain including the body interior. An implicit pressure correction method and multi-grid methods are used to integrate the governing equations. Steady and unsteady forced convection over a stationary circular cylinder and the natural convections over a heated circular cylinder embedded in a square cavity are computed this simple direct forcing method. The computed results generally compared well with published data.

REFERENCES

[1] Peskin C. S., The Immersed Boundary Method, *Acta Numerica*, 2002; 1-39.

[2] Goldstein D., Handler R. and Sirovich L., Modeling a No-Slip flow Boundary with an External Force Field, *J. Comput. Phys.*, 1993; **105**, 354-366.

[3] Saiki E. M. and Biringen S., Numerical Simulation of a Cylinder in Uniform Flow: Application of a Virtual Boundary Method, *J. Comput. Phys*, 1996; **123**, 450-465.

[4] Fadlun E.A., Verzicco R., Orlandi P. and Mohd-Yusof J., Combined Immersed-Boundary Finite-Difference Methods for Three-Dimensional Complex Flow Simulations, *J. Comput. Phys*, 2000; **161**, 35-60.

[5] Kim J., Kim D. and Choi H., An Immersed-Boundary Finite-Volume Method for Simulations of Flow in Complex Geometries, *J. Comput. Phys.*, 2001; **171**, 132-150.

[6] Baaijens Frank P.T., A Fictitious Domain/Mortar Element Method for Fluid-Structure Interaction, *Int. J. Numer. Meth. Fluids*, 2001; **35**, 743-761.

[7] D. Pan, "An Immersed Boundary Method for Incompressible Flows Using Volume of Body Function", *International Journal For Numerical Methods In Fluids*, Vol. 50, pp. 733-750, 2006..

[8] D. Pan, "An Immersed Boundary Method on Unstructured Cartesian Meshes for Incompressible Flows with Heat Transfer", *Numerical Heat Transfer, Part B, Fundamentals*, Vol. 49, pp. 277-297, 2006.

[9] C. Kiris and D. Kwak, "Numerical Solution of Incompressible Navier-Stokes Equations Using a Fractional-Step Approach," *Comp. & Flu*., Vol 30, pp. 829-851, 2001.

[10] A.L.F. Lima E Silva, A. Silverira-Neto, and J.J.R. Damasceno, "Numerical Simulation of Two-dimensional Flows over a Circular Cylinder Using the Immersed Boundary Method," *Journal of Computational Physics*, Vol. 89, pp. 351-370, 2003.

[11] Fornberg B.,A Numerical Study of Steady viscous Flow Past a Circular Cylinder, *J. fluid Mech.*, 1980, **98**, 819-855.

[12] J.R. Holman, *Heat Transfer*, fifth edition, pp. 243-244, McGraw-Hill, 1981.

[13] F. Moukalled and M. Darwish, "New Bounded Skew Central Difference Scheme, part II: Application to Natural Convection In An Eccentric Annulus," *Numerical Heat Transfer, Part B*, Vol. 31, pp. 111-133, 1997.

[14] H. Sadat and S. Couturier, Performance and Accuracy of a Meshless Method for Laminar Natural Convection, *Numerical Heat Transfer, Part B*, Vol 37, pp. 455-467, 2000.

Table I Simulation Results for Flows over a Circular Cylinder

Methods	Re	Cd	Lw/d	Cl	St	Nu
Current method	40	1.50	2.24			3.21
Pan(VOB)[7,8]	40	1.51	2.18			3.23
Fornberg [11]	40	1.50	2.24			
$0.911Re^{0.385}Pr^{1/3}$ [12]	40					3.36
Current method	100	1.32		± 0.32	0.164	4.99
Pan(VOB)[8]	100	1.32		± 0.32	0.160	5.02
Kim, Kim and Choi [5]	100	1.33		± 0.32	0.165	
$0.683Re^{0.466}Pr^{1/3}$ [12]	100					5.21

Table 2. Average Nusselt Number over a Heated Cylinder in Cavity, Radius=*0.1*, Center at *(0.35, 0.35)* from the left lower corner

Ra	Current Method	Pan (VOB) [7,8]	Moukalled and Darwish [13]	Sadat and Couturier [14]
10^4	*4.733*	*4.686*	*4.741*	*4.699*
10^5	*7.395*	*7.454*	*7.435*	*7.430*
10^6	*12.37*	*12.54*	*12.453*	*12.421*

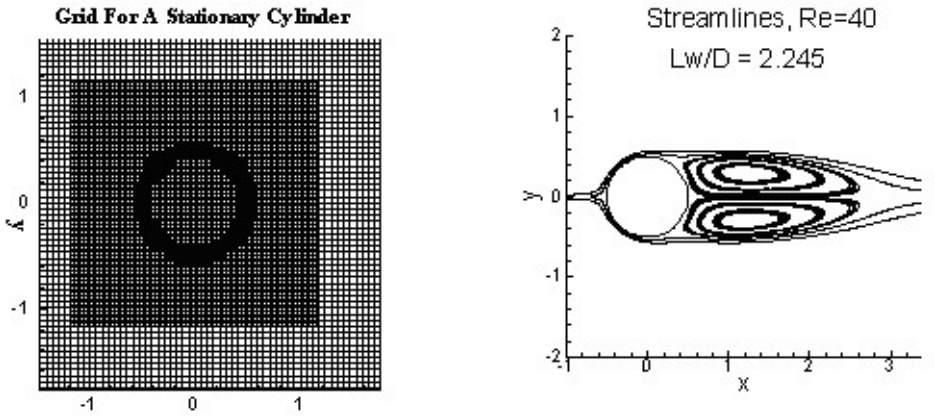

Fig. 1 Flows over a stationary circular cylinder, *Re*=40, (a) grid and (b) streamlines.

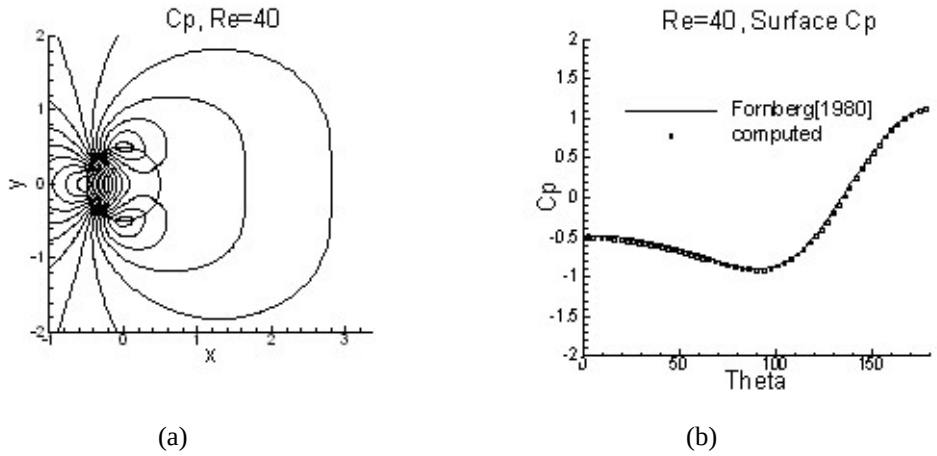

Fig. 2 Flows over a stationary circular cylinder, *Re*=40, (a) Cp contours, (b) Cp distribution around the cylinder surface, symbols: computed, line: Fornberg [11].

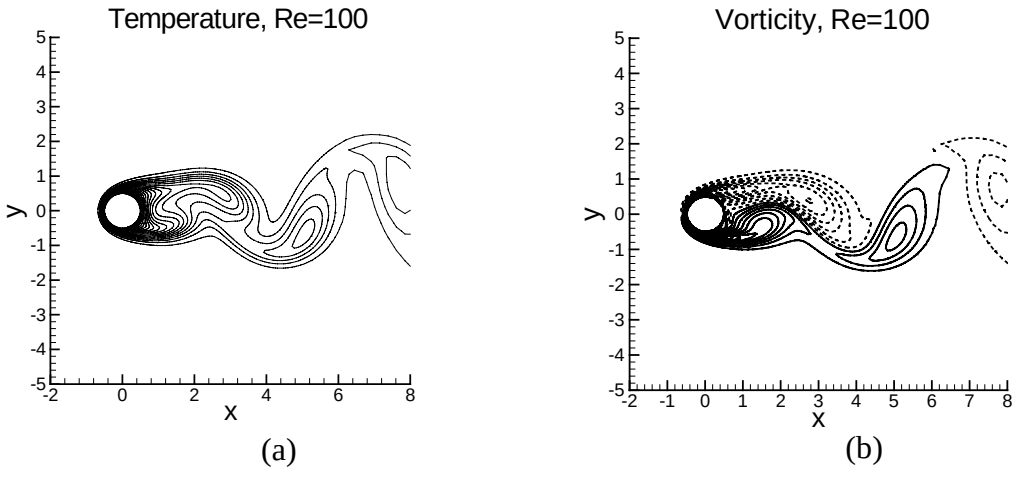

Fig. 3 Vortex shedding over a circular cylinder, *Re=100*, (a) temperature contours, (b) vorticity contours.

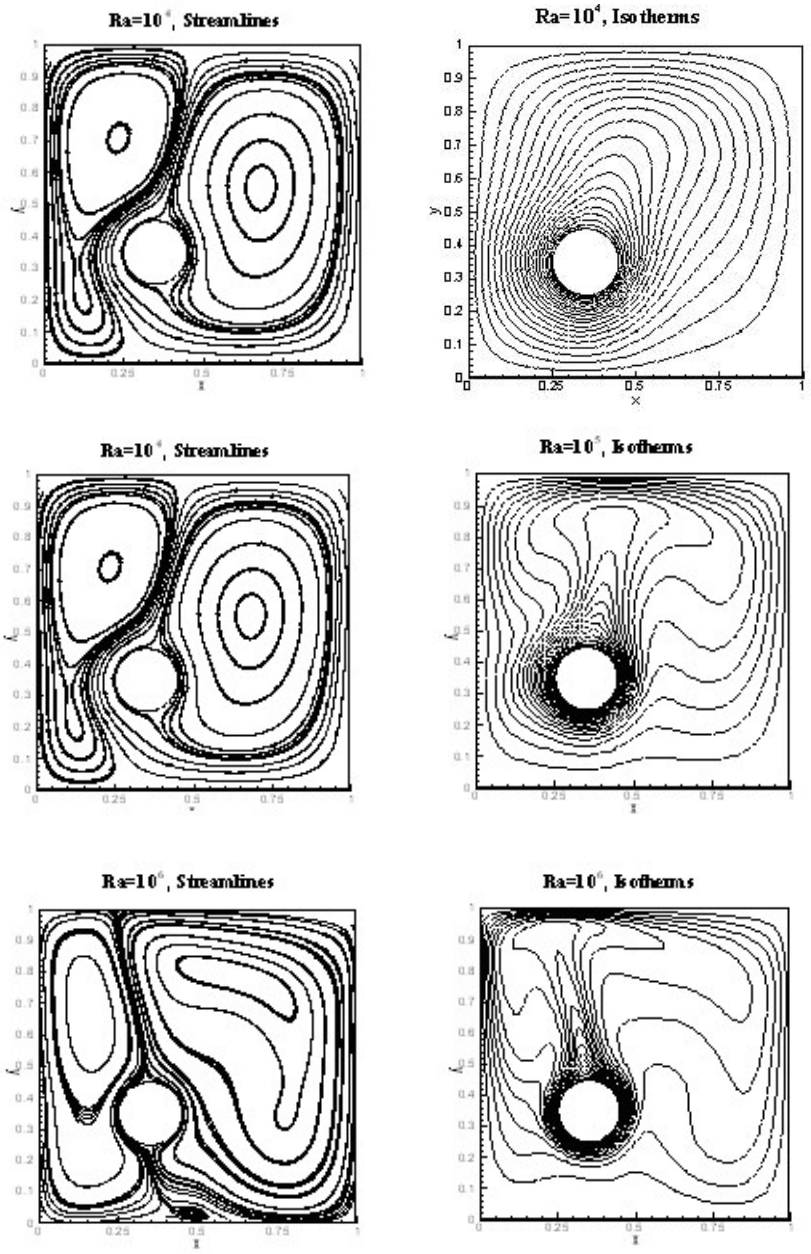

(a) (b)

Fig. 4 (a) Streamlines and (b) Isotherms for $Ra = 10^4$, 10^5 and $Ra = 10^6$